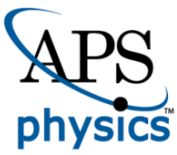

Multiple band structures in ^{70}Ge

R. A. Haring-Kaye, S. I. Morrow, J. Döring, S. L. Tabor, K. Q. Le, P. R. P. Allegro, P. C. Bender, R. M. Elder, N. H. Medina, J. R. B. Oliveira, and Vandana Tripathi

Phys. Rev. C **97**, 024308 — Published 7 February 2018

DOI: 10.1103/PhysRevC.97.024308

Multiple band structures in ^{70}Ge

R. A. Haring-Kaye,[1] S. I. Morrow,[2,*] J. Döring,[3] S. L. Tabor,[4] K. Q. Le,[1,†] P. R. P. Allegro,[5] P. C. Bender,[4,‡] R. M. Elder,[1,‡] N. H. Medina,[5] J. R. B. Oliveira,[5] and Vandana Tripathi[4]

[1]*Department of Physics and Astronomy, Ohio Wesleyan University, Delaware, Ohio 43015, USA*

[2]*Department of Physics, Houghton College, Houghton, New York 14744, USA*

[3]*Bundesamt für Strahlenschutz, D-10318 Berlin, Germany*

[4]*Department of Physics, Florida State University, Tallahassee, Florida 32306, USA*

[5]*Instituto de Física, Universidade de São Paulo, São Paulo, Brazil*

(Dated: December 22, 2017)

Abstract

High-spin states in ^{70}Ge were studied using the ^{55}Mn(^{18}O,$p2n$) fusion-evaporation reaction at a beam energy of 50 MeV. Prompt γ-γ coincidences were measured using the Florida State University Compton-suppressed Ge array consisting of three Clover detectors and seven single-crystal detectors. An investigation of these coincidences resulted in the addition of 31 new transitions and the rearrangement of four others in the ^{70}Ge level scheme, providing a more complete picture of the high-spin decay pattern involving both positive- and negative-parity states with multiple band structures. Spins were assigned based on directional correlation of oriented nuclei ratios, which many times also led to unambiguous parity determinations based on the firm assignments for low-lying states made in previous work. Total Routhian surface calculations, along with the observed trends in the experimental kinematic moment of inertia with rotational frequency, support the multi-quasiparticle configurations of the various crossing bands proposed in recent studies. The high-spin excitation spectra predicted by previous shell-model calculations compare favorably with the experimental one determined from this study.

PACS numbers: 21.10.Tg, 23.20.Lv, 27.50.+e

*Present address: Department of Physics and Astronomy, Vanderbilt University, Nashville, Tennessee 37235, USA.

†Present address: Department of Mathematics, Temple University, Philadelphia, Pennsylvania 19122, USA.

‡Present address: National Superconducting Cyclotron Laboratory, Michigan State University, East Lansing,

Michigan 48824, USA.

I. INTRODUCTION

The even-even Ge isotopes provide a fertile testing ground for a variety of exotic shape and structural properties. Recently, a study of ^{76}Ge revealed evidence for rigid triaxial deformation associated with the low-lying states of a γ-vibrational band based on the amplitude and phase of the $S(J)$ energy staggering parameter as a function of spin J [1]. The observed staggering pattern [$S(J)$ always larger for even J] is not only unique in the mass $A \approx 70$ region but is in fact very rare across the entire nuclear landscape. On the lighter side of stability, the ^{72}Ge isotope has presented several lingering questions surrounding its low-lying structure. In particular, understanding the structure and origin of its anomalous 0_2^+ first-excited state, atypical for even-mass nuclei far from closed shells, has remained elusive for many years. Only very recently has a possible explanation been put forth in terms of the degree of triaxiality and shape coexistence [2]. Even the possibility of highly-exotic excitation modes with tetrahedral symmetry has been explored in ^{72}Ge [3]. Although theoretical calculations [4] demonstrated that ^{72}Ge could have both a proton number ($Z = 32$) and neutron number ($N = 40$) located at a shell gap for α_{32} deformation (corresponding to tetrahedral symmetry), making ^{72}Ge a promising candidate for tetrahedral shapes, no experimental evidence was found for such structures [3].

Although not considered a candidate for the exotic shapes mentioned above, the stable ^{70}Ge isotope shows a rich structure with interesting similarities and differences compared to its neighboring even-even isotopes. Several low-spin ($J \leq 6$) studies were performed up to 5.1 MeV excitation energy using light-ion, transfer, and inelastic-scattering reactions [5–9]. Further insight into the low-spin structure was provided by a study of the β^+ decay of ^{70}As [10]. The earliest high-spin studies [11–13] revealed a complex decay scheme resulting from several different excitation modes associated with multi-quasiparticle (or multi-phonon) configurations, including a 3^- state at 2563 keV with possible octupole vibrational character [11]. The development of band structure was also evident from these works, including the first three states of a $K^\pi = 2^+$ γ-vibrational band. A high-spin band, based on the 3^- state near 2563 keV and reaching a (21^-) state at 13171 keV, was first reported over twenty years later using a more sensitive γ-ray spectrometer with recoil mass selectivity [14]. Nine years following this work, one new transition was added near the bottom of this band, three were removed at the top of the band, and two others were reordered in another in-beam study

[15]. The tentative negative-parity assignment was preserved, however. In addition, this study revealed a rotational band built on the 0_2^+ state (the second-excited state in ^{70}Ge), extending the sequence to an 8^+ state at 5431 keV. Very recently, a high-spin positive-parity band was observed up to a (20^+) state at 10268 keV (labeled as band B2), representing one of two even-spin branches above a forking of the ground-state band, and was attributed to a two-quasineutron configuration [16].

Despite these extensive experimental investigations, open questions and uncertainties cloud the interpretations of the observed decay structures in ^{70}Ge. The lowest odd-spin (signature $\alpha = 1$) negative-parity bands in neighboring ^{66}Ge [17], ^{68}Ge [18], and ^{72}Ge [3] each have a corresponding even-spin ($\alpha = 0$) signature partner, but so far an $\alpha = 0$ negative-parity band has not been found to accompany the band based on the 3^- state in ^{70}Ge. The $K = 2$ γ band has not been developed to as high a spin as in other neighboring even-even Ge isotopes, making it difficult to compare its characteristics to those of its neighbors in systematic fashion. Perhaps the most intriguing puzzle, however, involves the high-spin decay pattern. Previous versions of the level scheme [14, 15] show no linking transitions between the high-spin negative-parity band above the known $7^{(-)}$ state at 4296 keV and other known structures, casting lingering doubt about the ordering of its transitions. Curiously, a 626-keV $E2$ transition within this band, observed in Refs. [14] and [15], also appears in the new high-spin positive-parity band (band B2) shown in Ref. [16]. Negative-parity states are not reported in Ref. [16], so it is unclear if this transition represents a doublet in the level scheme or if it represents a rearranged placement.

The goal of this work was to carefully re-examine the high-spin decay of ^{70}Ge in order to resolve the puzzles that remain in this portion of the level scheme. As a result of this study, a candidate for an even-spin, negative-parity sequence was found, the $K = 2$ γ band was extended to higher spin, and a more complete picture of the high-spin decay structure (including both positive- and negative-parity states) was determined.

II. EXPERIMENTAL AND ANALYSIS METHODS

High-spin states in ^{70}Ge were populated by the ^{55}Mn(^{18}O,$p2n$) fusion-evaporation reaction at a beam energy of 50 MeV using the John D. Fox Superconducting Accelerator Facility at Florida State University (FSU). The $p2n$ channel comprised approximately 24% of the total

reaction cross section and represented the largest yield among several reaction products. The ^{55}Mn target had a thickness of 611 μg/cm^2 and was evaporated on to a 15 mg/cm^2 ^{197}Au backing to stop all recoils produced from the reaction.

The γ rays emitted from the reaction products were detected by an array of ten Compton-suppressed Ge detectors. Three Clover detectors and two single-crystal detectors were placed at 90° relative to the beam axis, and two (three) single-crystal detectors were placed at 35° (145°). Approximately 2.3×10^8 prompt γ-γ coincidences were recorded by the array under the condition that each two-fold (or higher) multiplicity event occurred within a time window of approximately 100 ns. These data were then sorted into a variety of γ-γ coincidence matrices with a dispersion of 0.8 keV/channel. Both the sorting and analysis of the γ-ray spectra were performed using GNUSCOPE, a γ-spectrum analysis software package developed at FSU [19, 20].

The γ-ray coincidences used to study the ^{70}Ge level scheme were investigated mostly with background-subtracted spectra projected from matrices of coincidences among the 90° detectors, in order to minimize Doppler shifting. Transition energies E_γ were determined by measuring the line centroids for the decays in as many clean gates as possible in the 90° coincidence spectra and averaging the results. Preliminary energy calibrations were obtained from an ^{152}Eu source, then modified to include a broader energy range based on the known energies of several clean γ-ray lines produced in beam. The γ-ray intensities were first determined at 90° either through clean gates on transitions below the lines of interest or from the total projection of 90° detector coincidences. They were then corrected for angular distribution effects using theoretical a_2 and a_4 coefficients determined from the spin change of the transition. These coefficients were utilized to deduce A_0, the angle-independent first-order term in the series of Legendre polynomials that describe the experimental intensities as a function of observation angle. Lastly, the A_0 values were normalized to the one obtained for the 1039.6-keV transition, resulting in a final relative intensity I_γ for each transition. The relative efficiency of the detectors as a function of E_γ was determined from the known intensities of a ^{152}Eu calibration source [21] and a standard logarithmic parameterization for Ge detectors. All measured γ-ray energies and intensities for ^{70}Ge are given in Table I.

Spin changes were measured for as many transitions in ^{70}Ge as possible based on directional correlation of oriented nuclei (DCO) ratios, defined according to:

$$R_{\rm DCO} = \frac{I_\gamma(\text{at } 35^\circ, 145^\circ;\ \text{gated by } \gamma_{\rm G} \text{ at } 90^\circ)}{I_\gamma(\text{at } 90^\circ;\ \text{gated by } \gamma_{\rm G} \text{ at } 35^\circ, 145^\circ)}. \quad (1)$$

In order to increase the statistics of the DCO ratio measurement, the analysis was performed using a matrix constructed to exploit the angular symmetry of the FSU Ge array, in which both 35° and 145° detector events were sorted against only the 90° detector events. Based on the geometry of the array, if the gate γ_G represents one or more stretched electric quadrupole ($E2$) transitions, then the DCO ratios for stretched $E2$ transitions as well as for $\Delta J = 0$ transitions are expected to be approximately unity, while $\Delta J = 1$ transitions yield ratios of about 0.5 if the mixing ratio δ is small [22]. All DCO ratios were measured by gating on stretched $E2$ decays. The results are shown in Table I and in most cases reflect weighted averages (based on the measurement uncertainty) of the values obtained from two or more gates.

III. THE LEVEL SCHEME

The level scheme of ^{70}Ge deduced from its high-spin population in the present work is shown in Fig. 1. Several other low-lying states in ^{70}Ge were observed following the β^+-decay of ^{70}As, which was also produced favorably in the experiment [23]. Although we were able to verify the low-spin decay spectrum from previous work [10], no new information was obtained from the β^+-decay of ^{70}As, so most of the associated states and transitions are not included in Fig. 1 for clarity. Overall, 31 new transitions were assigned to ^{70}Ge in this work, and four others have had their placement rearranged compared to the two most recent studies [15, 16]. The supporting evidence for these changes are discussed in the subsections that follow.

A. Ground-state band and associated band crossings

The yrast band of ^{70}Ge was established with firm spin-parity assignments up to an 8^+ state at 4204 keV using the ^{68}Zn(α,2n) reaction [11]. This work also extended this sequence up to a 5244-keV state (with unassigned spin and parity) by its decay to the 8^+ state through a 1040-keV transition very similar in energy to the ground-state transition from the 2_1^+ state. The yrast cascade was later verified up to the 8^+ state using the ^{60}Ni(^{12}C,2p) and

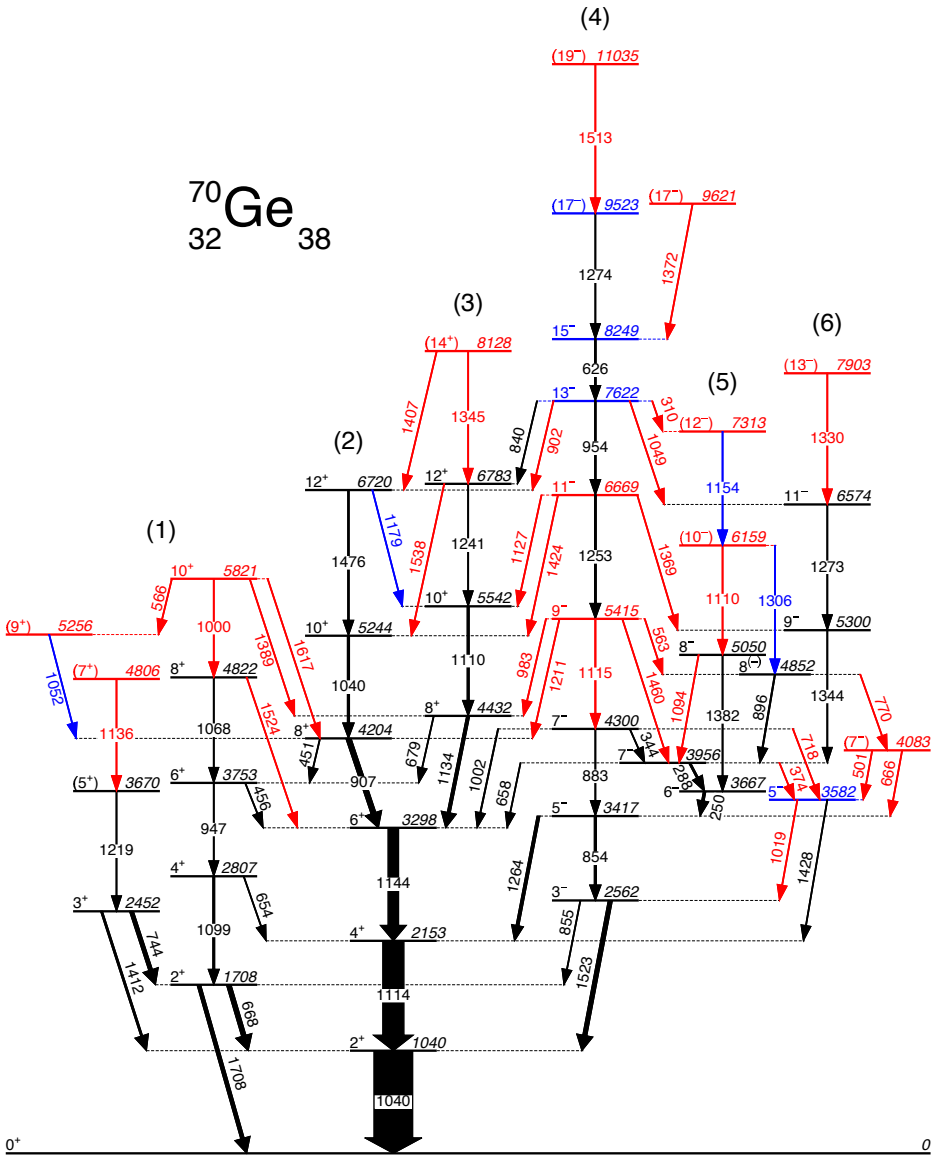

FIG. 1: (Color online) Partial level scheme of ^{70}Ge based on its population at high spin in the present work. Transitions and states shown in red (light grey) are new to this work, while those indicated in black have been verified from previous investigations. Transitions and states with either rearranged placements or new assignments compared with previous work are shown in blue (light grey). The numbers above each band sequence serve as labels used to facilitate the discussion in the text.

^{65}Cu(^{7}Li,2n) reactions [12]. Another high-spin study using the ^{46}Ti(^{28}Si,4p) reaction [14] confirmed the findings of Ref. [11]. More recently, the ^{60}Ni(^{12}C,2p) reaction was utilized to assign $J^{\pi} = 10^{+}$ to the 5244-keV state observed in Ref. [11], and to extend this band to

a 12^+ state at 6713 keV through the addition of a 1475-keV $E2$ transition above the 10^+ state [15]. The most recent high-spin study, using the ^{64}Ni(^{12}C,$\alpha 2n$) reaction, verified this structure up to the 12^+ state and extended it to a 14^+ state at 7765 keV with the observation of a 1051-keV transition at the top of the band [16].

Our work has confirmed these states and transitions up to the 12_1^+ level at 6720 keV, but we were unable to verify the placement of the 1051-keV γ ray (and the corresponding 14^+ parent state at 7765 keV) as observed in Ref. [16]. Our data are more consistent with a 1052-keV transition directly feeding the 8_1^+ state at 4204 keV, leading to a new level at 5256 keV. Further evidence for the 5256-keV state came from the observation of a 566-keV decay to this state from the 10_3^+ parent level at 5821 keV. Although a reliable DCO ratio could not be determined for either the 566- or the 1052-keV transition, a tentative spin-parity of (9^+) has been assigned to the 5256-keV state based on its similar excitation energy and decay as the 9^+ level at 5874 keV in ^{68}Ge [18]. Alternatively, the 5256-keV level could represent the 10_2^+ state, based on the measured DCO ratio of 1.17(12) for the 1051-keV γ ray in Ref. [16]. However, this possibility seems less likely given the lack of an observed $E2$ band above this state, contrary to the systematics in the neighboring Ge isotopes [3, 17, 18].

The ground-state band has been known to experience forking behavior above the 6_1^+ state for some time. Two nearly equally-populated 8^+ states were observed above the 6_1^+ level, each with a feeding transition that formed the start of an $E2$ band [11, 12]. As mentioned earlier, the yrast band (including the 8_1^+ state) has been confirmed up to a 12_1^+ state at 6720 keV. The yrare band based on the 8_2^+ level has consistently been observed up to a 5541-keV state in previous works, although with differing spin and parity assignments for this state [11, 12, 15]. Most recently, this particular band was extended to a (20^+) state at 10268 keV (corresponding to band B2 in Ref. [16]).

We observed a band structure (band (3) in Fig. 1) based on the 8_2^+ level at 4432 keV up to a (14^+) state at 8128 keV, supported in part by two new linking transitions of energy 1407- and 1538-keV observed between states in this band and the yrast band. Clear coincidences were seen between the low-lying $E2$ transitions associated with this band (1134, 1110, and 1241 keV) and γ rays with energy 840 and 626 keV, decays that were placed as the next two $E2$ transitions above the 12_2^+ state in Ref. [16]. However, our measured DCO ratio of 0.54(5) for the 840-keV transition, which disagrees with the value of 1.09(18) reported in Ref. [16], strongly suggests stretched dipole, rather than quadrupole, radiation. One way to

reconcile the two different DCO ratio measurements for this transition is to assume that it is a doublet, one with stretched dipole character and the other with stretched quadrupole character. However, the relatively weak intensity that we measured for the 840-keV line (see Table I) does not support this possibility, and none of the stretched $E2$ gates that were used to measure the DCO ratio of the 840-keV transition yielded a result consistent with quadrupole radiation. Our results for the 840-keV transition thus appear to be best described by a single $E1$ linking transition between high-spin negative-parity band (4) (see Sec. III C) and positive-parity band (3), as indicated in Fig. 1.

In addition, the 1178-keV line (measured with an energy of 1178.9(4) keV in this work), placed as a $18^+ \rightarrow 16^+$ transition in high-spin band B2 of Ref. [16], is reassigned as a linking transition between the 12_1^+ state at 6720 keV in yrast band (2) and the 10_2^+ state at 5542 keV in yrare band (3). This is based on the observed coincidence relations with the 1179-keV γ ray, the lack of mutual coincidences between 840- and 1179-keV decays (which were both placed in band B2 of Ref. [16]), and the measured energy difference between the 12_1^+ and 10_2^+ levels. Figure 2 shows a portion of the γ-ray coincidence spectra gated on the 840- (top) and 1179-keV (bottom) lines that give evidence for the new placement of the 1179-keV transition. As illustrated in the figure, the 840- and 1179-keV decays are not in coincidence with each other, and the 1179-keV gate does not show coincidences with the $12_2^+ \rightarrow 10_2^+$ 1241-keV transition (as would be the case in the decay scheme of Ref. [16]). Moreover, we could not place an 846-keV transition, given as the $(20^+) \rightarrow 18^+$ transition in band B2 of Ref. [16], in our level scheme.

B. $K = 2$ γ-vibrational band

The two sequences of states labeled as band (1) in Fig. 1 have a band-head energy (1708 keV), energy spacings, and decay pattern characteristic of other γ-vibrational bands in this mass region. Previous studies observed this band structure up to a (6^+) state at 3754 keV in the favored sequence [11, 12], and a state at 2452 keV with a firm 3^+ assignment [11]. Another level was identified at 3670 keV by its decay to the 3^+ state through a 1218-keV transition, but no spin-parity assignment was given [11]. These states were later verified, with the exception of the one at 3670 keV [15]. The most recent study extended the favored $\alpha = 0$ sequence to an (8^+) state at 4819 keV, and found agreement with Ref. [11] by including

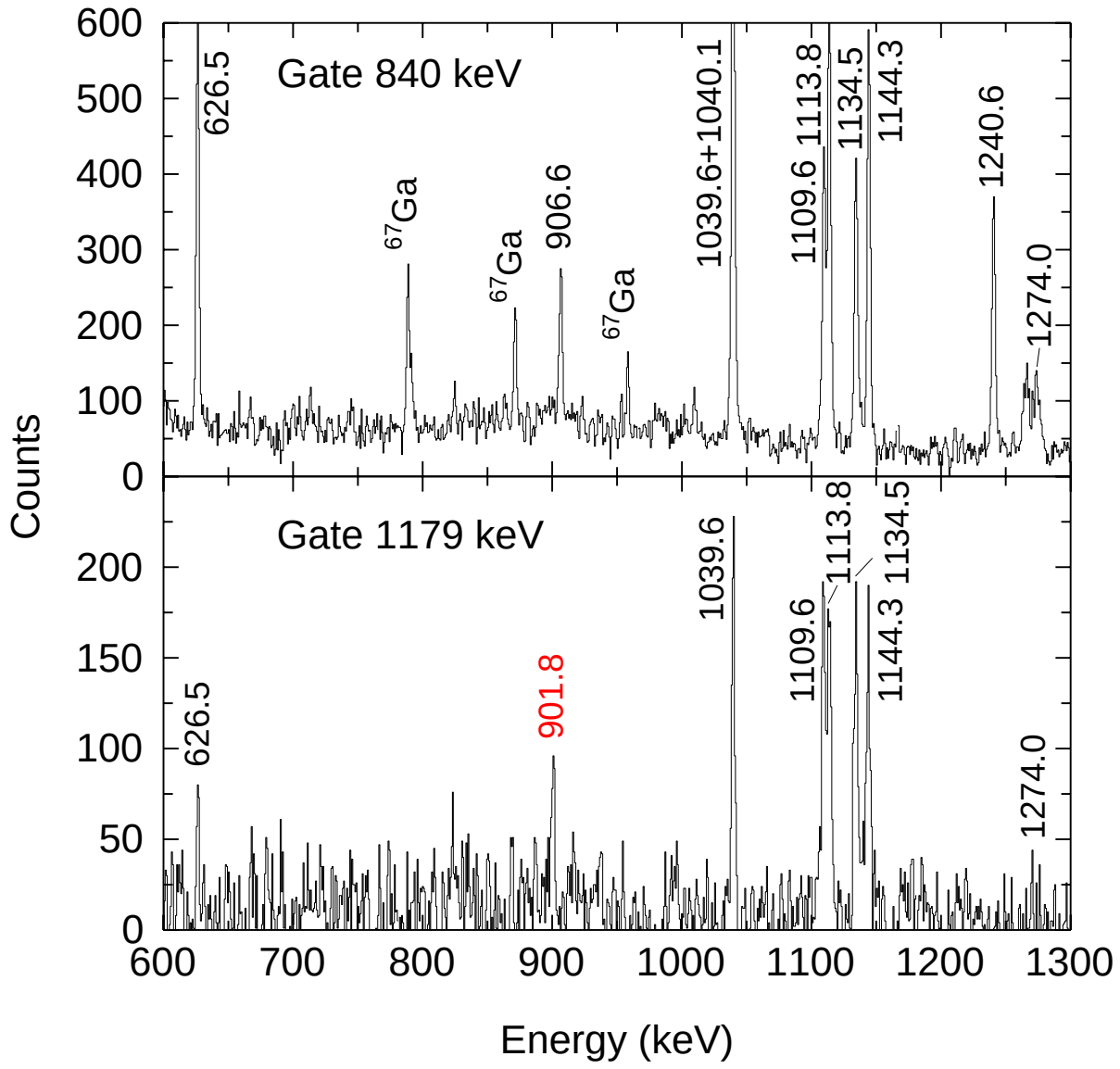

FIG. 2: (Color online) A portion of the 90° background-subtracted coincidence spectra obtained by gating on 840- (top) and 1179-keV (bottom) γ rays. The 901.8-keV line is labeled in red (or light grey) to indicate that it is a new transition in the ^{70}Ge level scheme determined from this work.

a state at 3668 keV with a tentative (5^+) assignment as part of the unfavored $\alpha = 1$ cascade [16].

We have verified the levels and transitions within this structure as observed in Ref. [16], and have extended the band up to a 10_3^+ state at 5821 keV in the $\alpha = 0$ sequence and a (7^+) state at 4806 keV in the $\alpha = 1$ cascade. Coincidence gates on 744- and 1099-keV γ rays, shown in Fig. 3, indicate evidence for the 1000- and 1136-keV decays that have been

placed at the top of the even- and odd-spin sequence, respectively. New linking transitions of energy 1389, 1524, and 1617 keV found between the favored sequence and other established levels provide further support for the 8_3^+ and 10_3^+ states. Firm spin-parity assignments of 8_3^+ and 10_3^+ have been given to the states at 4822 and 5821 keV, respectively, based on the measured DCO ratios of the 1000-, 1068-, 1389-, and 1617-keV transitions (see Table I). The transitions in the odd-spin sequence above the 3^+ state were too weak to infer a spin change from their DCO ratios, so the spin assignments remain tentative above this level.

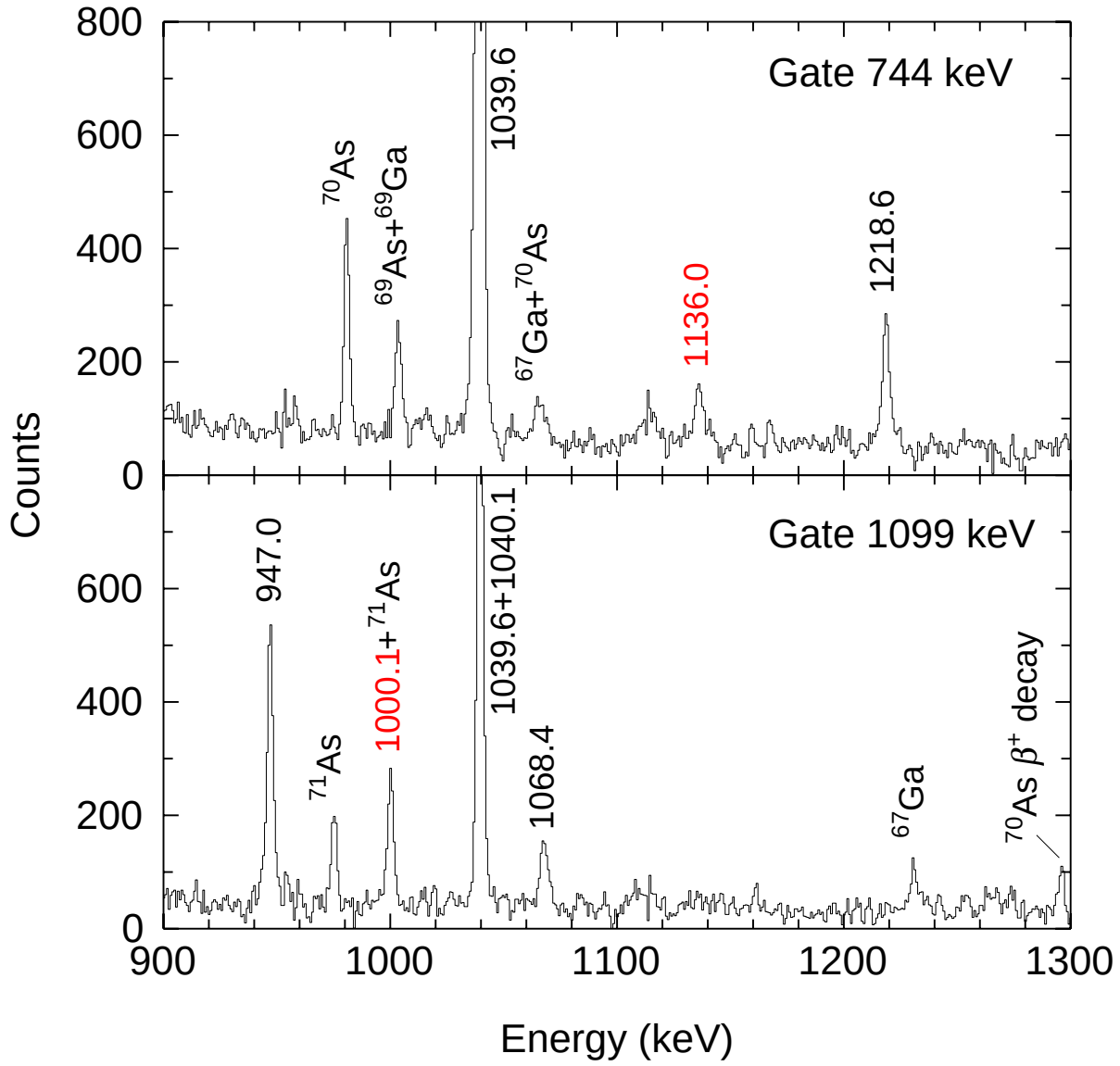

FIG. 3: (Color online) A portion of the 90° background-subtracted coincidence spectra obtained by gating on 744- (top) and 1099-keV (bottom) γ rays. New transitions in the ^{70}Ge level scheme, as determined from this work, have their energies labeled in red (or light grey).

C. Negative-parity bands

Several low-spin negative-parity states in ^{70}Ge were identified from the earliest studies of this nucleus using light-projectile reactions [5–9, 11], heavy-ion reactions [12, 13], and a more recent investigation of the β^+ decay of ^{70}As [10]. The lowest state with negative parity was first identified as the one at 2562 keV [8] with a likely spin of $J = 3$ [6]. An angular distribution and linear polarization measurement of the 1523-keV transition to the 2_1^+ state at 1040 keV established $E1/M2$ character for this decay and provided a firm 3^- assignment for the 2562-keV level [24]. The first high-spin band structure that was (tentatively) assigned negative parity was revealed by Ref. [14], indicating a band based on the 3^- state that reached a (21^-) level at 13171 keV. Interestingly, a $7^- \rightarrow 5^-$ transition was missing from the observed $E2$ cascade. Later, a similar high-spin sequence, again with a tentative negative-parity assignment, was reported in Ref. [15]. This band was also based on the 3^- state at 2561 keV, but incorporated a different $7^{(-)}$ state as part of the cascade (a state at 4296 keV that was also observed in Ref. [14]), and included a 882-keV intraband transition between this $7^{(-)}$ state and a $5^{(-)}$ state at 3414 keV. Above the $7^{(-)}$ level, this work also extended the band with $E2$ transitions of energy 1252, 952, 625, and 1272 keV (in that order with increasing excitation energy) up to a $15^{(-)}$ state at 8396 keV, representing a reversal in the order of the 953- and 1252-keV transitions and a reduction of the total number of transitions observed in this band compared to Ref. [14]. Negative-parity states were not reported in the most recent high-spin investigation of ^{70}Ge [16].

The γ-ray coincidence relations and relative intensities observed in this work confirm the negative-parity excitation spectrum reported in Ref. [15] up to the 7_2^- state at 4300 keV (including a 6_1^- state at 3667 keV and the 7_1^- state at 3956 keV). A state at 3582 keV, observed previously with an energy of 3581.3 keV from an experiment utilizing the $(n,n'\gamma)$ reaction [25], was confirmed by its 1428-keV decay as well as the discovery of new 374-, 501-, 718-, and 1019-keV transitions (see Fig. 1). Although a spin-parity of 4^+ was given to this state previously [25], our firm 5^- assignment is based on the measured DCO ratio of 1.04(37) for the 1019-keV transition, which almost certainly corresponds to $E2$ decay to the 3^- state at 2562 keV. Additional confirmation of the 5^- assignment comes from the measured DCO ratio of 0.58(12) for the 1428-keV transition, consistent with $E1$ decay to the 4_1^+ state. Furthermore, a new state was placed at 4083 keV based on the observation of

501-, 666-, and 770-keV transitions that link this state to other known levels. A tentative assignment of $J^\pi = (7^-)$ has been proposed by analogy to the triplet of 7^- states that occur in ^{66}Ge [17] and ^{68}Ge [18] within a similar range of excitation energies.

Above the 7_3^- state, our data reveal a new 9^- state at 5415 keV, confirmed by its decay to both positive- and negative-parity levels through the observation of 563-, 983-, 1115-, 1211-, and 1460-keV γ rays (see Fig. 1). Such a fragmented decay pattern from a well-populated, high-spin level with negative parity, which forms part of a band based on the lowest 3^- state, has also been observed in ^{66}Ge [17] and ^{68}Ge [18]. The spin and parity of this new 9_2^- state were inferred from the measured DCO ratios of the 563-, 1115- and 1211-keV transitions that depopulate this state. The measured DCO ratio of 0.91(25) for the 1115-keV transition (obtained by gating on 854-keV γ rays to eliminate contamination from the much stronger $4_1^+ \rightarrow 2_1^+$ 1114-keV line) strongly suggests quadrupole (and therefore almost certainly $E2$) decay to the 7_3^- state at 4300 keV. The 9^- assignment is also consistent with the measured DCO ratio of 0.44(6) [0.57(26)] for the 1211-keV [563-keV] transition, which implies stretched dipole decay to the 8_1^+ [$8_1^{(-)}$] state at 4204 keV [4852 keV]. The 983- and 1460-keV decays were too weak, however, to allow a precise determination of their DCO ratios and provide further confirmation of the spin-parity assignment for the 9_2^- state. Above the 9_2^- level, an odd-spin band structure consisting of $E2$ transitions (inferred from measured DCO ratios) was found that matches the same sequence of transitions observed in Ref. [15] above the 7_3^- state, and includes an additional 1513-keV decay that extends the cascade to a (19^-) state at 11035 keV (band (4) in Fig. 1). Linking transitions of energy 310, 840, 902, 1049, 1127, 1369, and 1424 keV from states in this high-spin sequence to other excited states firmly establish the excitation energies, and in some cases confirm the spin-parity assignments, for many of these levels. Figure 4 shows a coincidence spectrum obtained by gating on 854-keV γ rays, indicating many of the transitions in band (4) along with several others that are also associated with the decay of negative-parity states in ^{70}Ge.

Even-spin negative-parity bands have been observed in ^{66}Ge [17], ^{68}Ge [18], and ^{72}Ge [3], but so far have remained elusive in the study of ^{70}Ge. These bands are typically less strongly populated than the favored odd-spin negative-parity bands that have been observed up to high spin, which could explain why no such even-spin sequence has yet been observed in ^{70}Ge. Until now, the only viable candidates for even-spin negative-parity excitation above 4 MeV have been an $8^{(-)}$ state at 4853 keV [12, 15] and a level at 5300 keV [12], without

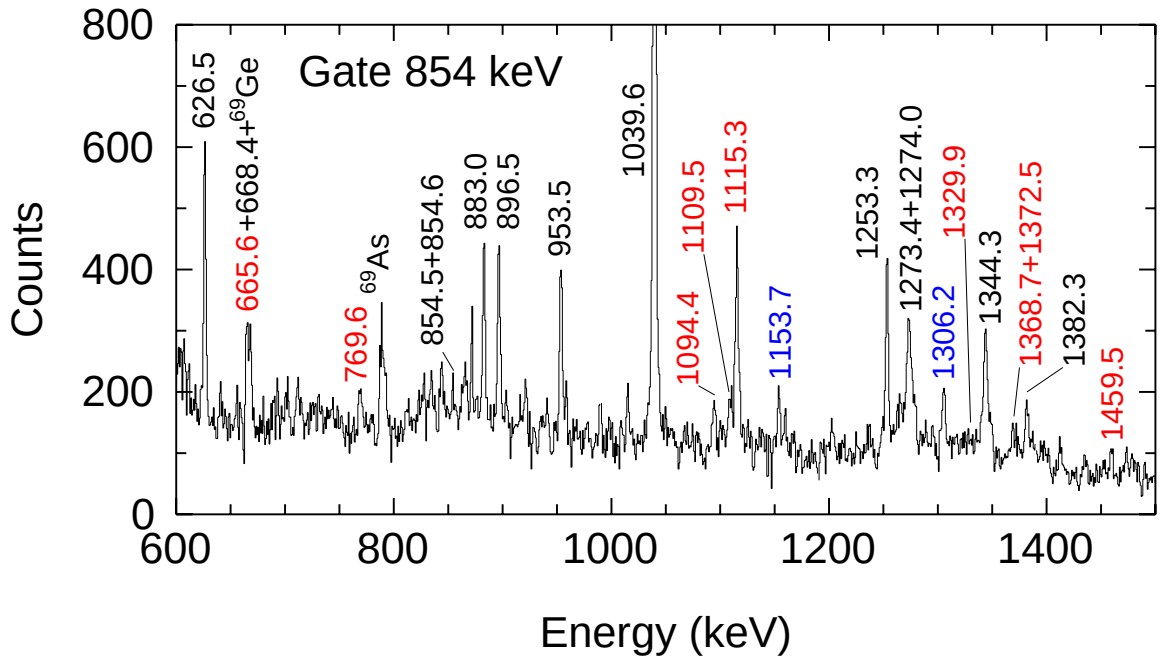

FIG. 4: (Color online) A portion of the 90° background-subtracted coincidence spectra obtained by gating on 854-keV γ rays. New (Rearranged) transitions in the ^{70}Ge level scheme, as determined from this work, have their energies labeled in red (blue) or light grey.

any apparent band structure.

Our work has likely identified an even-spin negative-parity band for the first time in ^{70}Ge, based on the 6^- state at 3667 keV and extending up to a (12^-) state at 7313 keV (band (5) in Fig. 1). The 8^- member of this band, at 5050 keV, has been reported once before [11] (without a spin-parity assignment) through its decay to the 6^- state at 3667 keV by a 1382-keV transition. The observation of a new 1094-keV depopulating transition to the 7^-_1 state at 3956 keV now provides additional confirmation for the level at 5050 keV. A firm 8^- assignment for the 5050-keV state is based on the measured DCO ratio of 1.02(24) for the 1382-keV transition (indicating $E2$ character) to the 6^- state at 3667 keV. The higher-lying states in this band, a (10^-) state at 6159 keV and a (12^-) state at 7313 keV, were deduced in part from their decay by two transitions (1154 and 1306 keV) that were observed previously [14] but placed differently in the ^{70}Ge level scheme. Both the (10^-) and (12^-) states have a linking transition to (or from) another known level to confirm their placements.

Two other levels at 4852 and 5300 keV were reported in Ref. [11] without spin-parity assignments. Tentative assignments of (8^-) and $(6^-, 7^-, 8^-)$ were given for the 4852 and

5300 keV states, respectively, in Ref. [12] based on the measured angular distributions of the 897- and 1344-keV depopulating transitions. An $8^{(-)}$ [$9^{(-)}$] assignment was given for the 4852-keV [5300-keV] state in Ref. [15] based on the measured DCO ratio of the 896-keV [1343-keV] transition. The DCO ratios of the 896- and 1344-keV transitions measured in this work (see Table I) are consistent with those measured in Ref. [15], and thus provide confirmation of the spin-parity assignments for the 4852- and 5300-keV states given in this work. Transitions of energy 1273 and 1330 keV were observed to be in coincidence with the 1344-keV decay as well as each other, confirming another odd-spin negative-parity sequence observed previously up to an $11^{(-)}$ state at 6567 keV [15] (6574 keV in this work), and extending it to a new (13_2^-) state at 7903 keV (band (6) in Fig. 1). The measured DCO ratio of 0.88(22) for the 1049-keV transition from the 13_1^- parent state at 7622 keV very likely corresponds to $E2$ decay and thus provides a firm 11^- assignment for the 6574-keV state in this band.

D. Excited 0_2^+ band

Low-lying excited 0^+ states are common among the even-even Ge isotopes, and ^{70}Ge is no exception. The 0_2^+ state in ^{70}Ge has been known since the earliest studies of this nucleus [5–9], and was later confirmed using fusion-evaporation reactions [13]. Higher-lying 2_3^+ and 4_3^+ states were found to decay to the 0_2^+ state through a sequence of γ rays with energy 941.10 and 901.95 keV following the β^+ decay of ^{70}As [10], providing confirmation of the 4_3^+ state observed in Refs. [11–13]. More recently, a rotational band based on the 0_2^+ state was reported up to a 8^+ state at 5430 keV [15].

We were able to confirm the states in this band structure up to the 4_3^+ level as given in Ref. [15]. The state near 4100 keV, given with $J^\pi = 6^+$ in Ref. [15], could also be confirmed based on its decay to the 4_2^+ level by a 1295-keV transition and to the 4_1^+ level via a weak 1948-keV transition. (We could not conclusively verify the 688- and 1044-keV depopulating transitions, though.) However, a 4102-keV state was observed following the β^+ decay of ^{70}As, including 1295- and 1948-keV depopulating transitions to the states mentioned above, with an assignment of $J = (3, 4)$ [10]. In addition, we could not verify the 8^+ state near 5430 keV first reported in Ref. [15]. This seems to suggest that the states belonging to the 0_2^+ band are populated primarily from the β^+ decay of ^{70}As, and are only very weakly

populated (if at all) from the high-spin decay of ^{70}Ge. Therefore, they are not included as part of the high-spin decay scheme shown in Fig. 1.

IV. DISCUSSION

The observed high-spin level structure of ^{70}Ge, including both positive- and negative-parity states, has been interpreted in terms of shell-model calculations utilizing an extended $P+QQ$ interaction with monopole interactions (EPQQM) as well as an effective interaction developed from a renormalized G matrix [15]. More recently, positive-parity band structures, including a proposed γ band based on a two-quasiparticle (2-qp) configuration, were discussed within the context of cranked shell-model (CSM) and triaxial projected shell-model (TPSM) predictions [16]. States in ^{70}Ge below an excitation energy of 8 MeV were also predicted by shell-model calculations with the PMMU effective interaction in a systematic application to nuclei in the $pf_{5/2}g_{9/2}$ shell region [26]. Other systematic comparisons across the even-even Ge isotopes (including ^{70}Ge) have been performed recently using a variety of theoretical approaches, including investigations of the degree of collectivity at low spin [27, 28] and the shape evolution from γ-soft to γ-rigid spanning the $^{70-80}$Ge chain [29].

Since the high-spin band structure of ^{70}Ge has been modified significantly in the present work, the implications of these changes on their interpretation within the framework of these theoretical approaches will be discussed when applicable. Total Routhian surface (TRS) calculations following the cranked Woods-Saxon approach [30] were also performed in order to predict the degree of collectivity in the new band structures observed in this work, and to see if shape changes are correlated with the qp alignments identified from CSM calculations. The results of these various interpretive calculations are described in the subsections that follow, organized according to the band structures illustrated in Fig. 1.

A. Ground-state band and associated band crossings

The low-lying yrast positive-parity states in ^{70}Ge have been interpreted in terms of random phase approximation (RPA) calculations obtained from a boson expansion approach [31], the Interacting Boson Model (IBM) with configuration mixing [32], and the EXCITED VAMPIR approach [33]. The models provided reasonable agreement between the predicted

excitation spectrum and the measured one up to an energy of about 3 MeV as long as significant configuration (or shape) mixing was incorporated in the calculations. In particular, the EXCITED VAMPIR results indicated strong mixing of prolate and oblate intrinsic qp determinants, implying an insensitivity to the triaxiality shape parameter γ. This picture is consistent with TRS calculations performed for the vacuum configuration in ^{70}Ge, as illustrated in Fig. 5. At a rotational frequency of $\hbar\omega = 0$ MeV (top panel of Fig. 5), the calculations reveal a strongly γ-soft shape. The absolute minimum energy in the surface, which likely corresponds to the ground state, occurs at a quadrupole deformation of $\beta_2 = 0.23$ and $\gamma = -71°$, indicating a moderate-deformed, near-oblate shape. This minimum persists up to $\hbar\omega \approx 0.3$ MeV in the calculations, consistent with a measurement of the static quadrupole moment $Q_{2^+} = +0.03(6)$ or $+0.09(6)$ eb for the 2_1^+ state [34]. At $\hbar\omega = 0.5$ MeV, approximately the frequency of the first band crossing (see below), the TRS shows a more pronounced minimum at $\beta_2 = 0.34$ and $\gamma \approx 3°$ (middle panel of Fig. 5), which persists to higher frequencies in fair agreement with previous TRS calculations [16]. This stabilization toward nearly-prolate deformation might be due to the $N = 38$ shell gap that exists for prolate deformation in the Nilsson single-particle energy spectrum, as discussed in Ref. [3]. Shapes with $\gamma \approx +10°$, predicted to occur near $\hbar\omega = 0.7$ MeV in previous TRS calculations and associated with a loss of collectivity [16], do not occur until $\hbar\omega \approx 0.8$ MeV in our calculations (bottom panel of Fig. 5).

The predicted shape change near $\hbar\omega \approx 0.5$ MeV occurs at the approximate frequency at which the first band crossing takes place in the ground-state band, attributed to a $g_{9/2}$ neutron alignment [11, 12, 15, 16]. As illustrated in the top panel of Fig. 6, which shows experimental kinematic moments of inertia $J^{(1)}$ as a function of rotational frequency, low-lying band crossings are a universal feature of the ground-state bands in the $^{66-72}$Ge isotopes, although the crossing frequency decreases with increasing N. A similar systematic trend was observed for the 2-qp bands based on the $(\nu h_{11/2})^2$ configuration in the Xe isotopes, attributed to an increase of the β_2 prolate deformation [35]. An analogous situation may be occurring in the Ge isotopes as neutrons fill the downsloping orbitals of the $g_{9/2}$ shell at prolate deformation.

The microscopic origins of the ground-state band crossings in the $^{66-72}$Ge isotopes are not always clear since valence protons and neutrons occupy the same orbitals in these nuclei and thus align at similar rotational frequencies. However, both shell-model calculations [15]

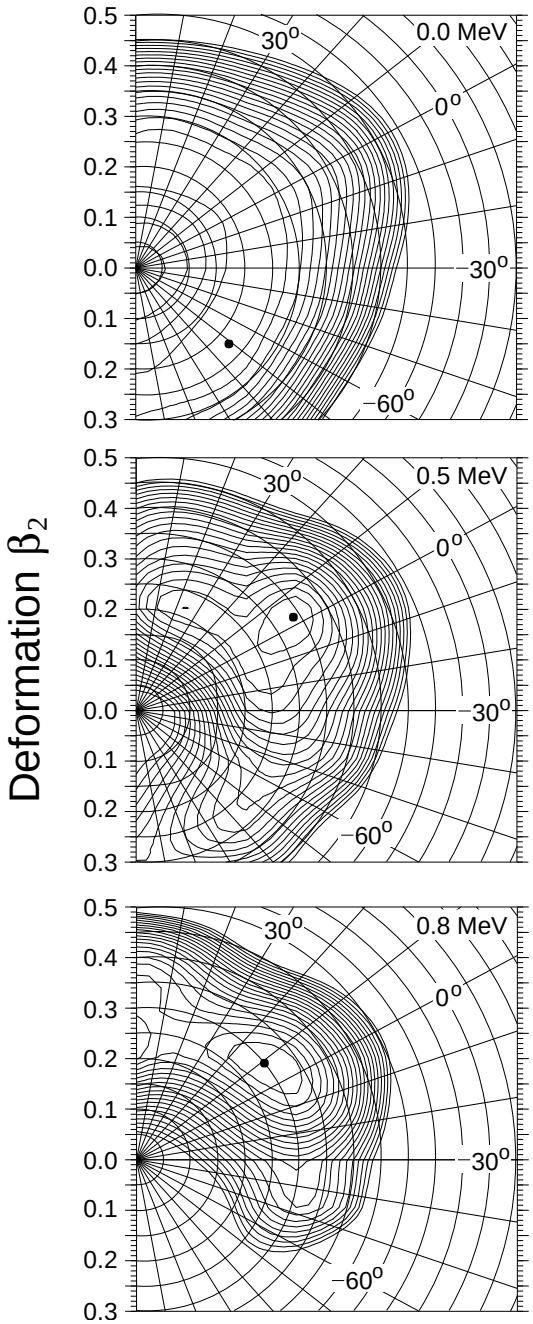

FIG. 5: Sample total Routhian surfaces in the (β_2, γ) plane for the vacuum configuration in ^{70}Ge at rotational frequencies of $\hbar\omega = 0$ (top), 0.5 (middle), and 0.8 MeV (bottom). The spacing between contour lines is 200 keV.

and quasiparticle Routhians calculated for $\beta_2 = 0.27$ and $\gamma = -15^\circ$ [16] unambiguously indicated that a $g_{9/2}$ quasineutron alignment is very likely associated with the band crossing near 0.5 MeV in ^{70}Ge, leading to a $(\nu g_{9/2})^2$ assignment for the 8_1^+ state and the yrast band built upon it (band (2) in Fig. 1). The same conclusion was reached for the first ground-state

band crossing in ^{72}Ge based on CSM calculations [3].

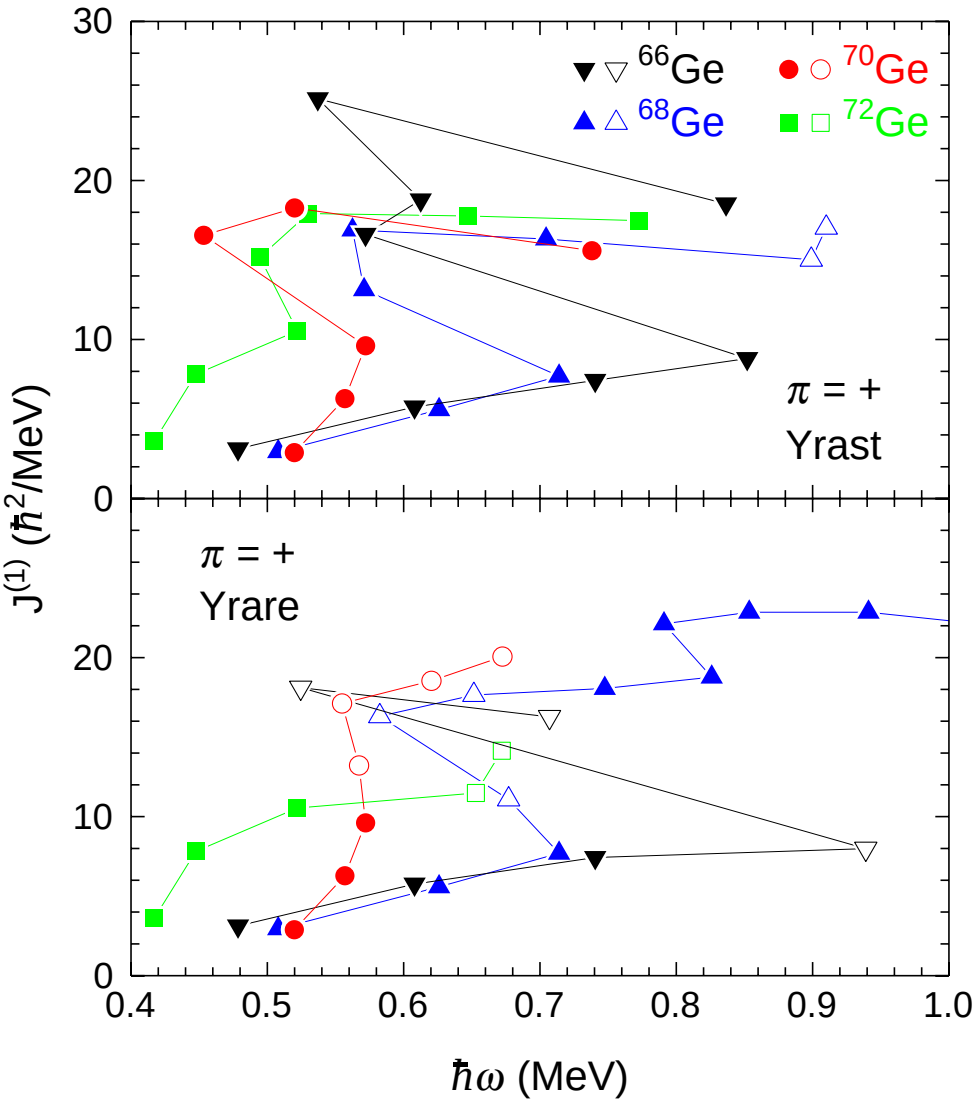

FIG. 6: (Color online) Experimental kinematic moments of inertia $J^{(1)}$ as a function of rotational frequency for the ground-state band and its progression to even-spin yrast (yrare) bands based on the 8_1^+ (8_2^+) state in ^{66}Ge [17], ^{68}Ge [18], ^{70}Ge, and ^{72}Ge [3], as indicated in the upper (lower) panel. Filled (open) symbols represent transitions with yrast (yrare) parent states. A common value of $K = 0$ was used for each band.

Forking behavior above the 6_1^+ state is also a common feature among the $^{66-72}$Ge isotopes, although their characteristics are somewhat different. Each of these isotopes exhibit relatively strong feeding from an 8_2^+ state to the 6_1^+ state (although not as strong as from the 8_1^+ state). In ^{66}Ge, however, the yrast band was observed to split into two $\Delta J = 2$

sequences connected by $\Delta J = 1$ $M1$ transitions, a structure suggested to be based on a deformed $(\pi g_{9/2})^2(\nu g_{9/2})^2$ 4-qp configuration [17]. In this isotope, the 8_2^+ state is associated with a $K = 2$ γ-vibrational band and lies below the onset of the high-spin $M1$ sequence. On the other hand, the 8_2^+ state in ^{68}Ge forms the start of a rather strongly-populated yrare $E2$ sequence separate from the γ-vibrational band, and becomes yrast above the 12_2^+ state [18]. There may be an onset of a similar yrare sequence based on the 8_2^+ state in ^{72}Ge [3], although so far only one $E2$ transition has been observed in this structure. Given these characteristics, the forking behavior above the 6_1^+ state in ^{70}Ge appears to be more similar to that in ^{68,72}Ge than in ^{66}Ge. Still, the behavior of $J^{(1)}$ for the yrare bands in ^{66,68,70}Ge seems most consistent with each other over the frequency range in which they can be compared, as shown in the bottom panel of Fig. 6, and could point to a possible similarity in the underlying structure of these bands.

One of the first interpretations of the two lowest 8^+ levels in ^{68,70}Ge, based in terms of two quasiparticles coupled to a weakly deformed core, suggested that one was based on two aligned $g_{9/2}$ neutrons and the other on two aligned $g_{9/2}$ protons [12, 36]. This analysis further predicted that there would be bands built on these states with energy spacings comparable to those of the ground-state band. Subsequent particle-plus-rotor calculations in ^{68}Ge [37] favored a $(\nu g_{9/2})^2$ assignment for the 8_1^+ state and $(\pi g_{9/2})^2$ for the 8_2^+ state, whereas the $(\nu g_{9/2})^2$ configuration was proposed for the 8_2^+ state [38, 39] based on EXCITED VAMPIR calculations for high-spin states [40, 41]. The contrasting pictures presented by these different theoretical descriptions is likely a reflection of the strong competition between quasineutron and quasiproton alignments in the Ge isotopes. Despite this ambiguity, neutron character was established for both the 8_1^+ and 8_2^+ states in ^{68}Ge based on a g-factor measurement for these levels [42].

Very recently, the 8_2^+ state in ^{70}Ge (and the proposed high-spin band built upon it) was suggested to be based on a $(\nu g_{9/2})^2$ configuration, based in part on an observed alignment near $\hbar\omega \approx 0.53$ MeV that was consistent with the predicted band crossing frequency for quasineutrons [16]. However, since the observed $14^+ \rightarrow 12_2^+$ transition energy in this band is significantly larger in our work, the sharp alignment observed at $\hbar\omega \approx 0.53$ MeV in Ref. [16] is no longer evident, as indicated in the bottom panel of Fig. 6. Rather, a more gradual alignment appears to be occurring toward $\hbar\omega \approx 0.6$ MeV, providing better agreement with TPSM predictions that assume a two-quasineutron configuration [16]. Also, the trend in

$J^{(1)}$ for this yrare band now shows better agreement with the analogous band in ^{68}Ge (based on the $(\nu g_{9/2})^2$ configuration) above the crossing frequency (lower panel of Fig. 6). Thus, our results appear to be consistent with the suggestion [16] of $(\nu g_{9/2})^2$ character for the 8_2^+ state and the band based upon it (band (3) in Fig. 1). Although the 8_2^+ state could instead be based on the $(\pi g_{9/2})^2$ configuration, recent CSM calculations [16] predict a significantly higher frequency for the lowest proton alignment ($\hbar\omega \approx 0.75$ MeV) than the frequencies associated with the observed ground-state band crossings. Moreover, TRS calculations for the vacuum configuration at frequencies near and above the lowest observed alignment do not reveal secondary collective minima that compete favorably with the lowest one (see Fig. 5). Additional TRS calculations performed for the lowest available two-quasineutron configuration yielding states with $\alpha = 0$ and $\pi = +$, which could correspond to a $(\nu g_{9/2})^2$ band, indicate an absolute energy minimum at $\beta_2 \approx 0.32$ and $\gamma \approx 5^\circ$ at $\hbar\omega \approx 0.6$ MeV (just above the lowest crossing frequency), very similar to the deformation parameters associated with the minimum energy of the vacuum configuration at the same frequency ($\beta_2 \approx 0.34$ and $\gamma \approx 3^\circ$). By comparison, TRS calculations that most likely correspond to a $(\pi g_{9/2})^2$ band favor a shape with a somewhat smaller quadrupole deformation ($\beta_2 \approx 0.28$) and larger positive γ values ($\gamma \approx 11^\circ$) at this frequency.

B. $K = 2$ γ-vibrational band

The first-excited positive-parity band in ^{70}Ge (band (1) in Fig. 1) shares several characteristics common to the low-lying γ-vibrational bands in other neighboring nuclei. The excitation energy of the 2^+ bandhead state is less than 700 keV above the yrast 2_1^+ level, likely precluding a multi-qp configuration. The relatively large measured $B(E2)$ value of 64(11) W.u. for the 668-keV $2_2^+ \rightarrow 2_1^+$ transition [43] implies substantial collectivity. The behavior of the static moment-of-inertia parameter $\mathcal{I}$ as a function of spin J, defined by [44]

$$\frac{2\mathcal{I}}{\hbar^2} = \frac{4J - 2}{E_J - E_{J-2}}, \tag{2}$$

for both the $\alpha = 0$ and the $\alpha = 1$ sequence of this structure is very similar to that of other known γ bands in the neighboring even-even Ge isotopes, as illustrated in Fig. 7. The steep rise in $\mathcal{I}$ with spin (or rotational frequency) is consistent with the expectation for vibrational excitations [46]. Furthermore, the measured excitation energies of the states

in band (1) compare favorably with those associated with a $K = 2$ γ vibration in TPSM calculations [16]. All of these features of band (1) strongly suggest that it represents a γ vibration, as implied previously [16, 47].

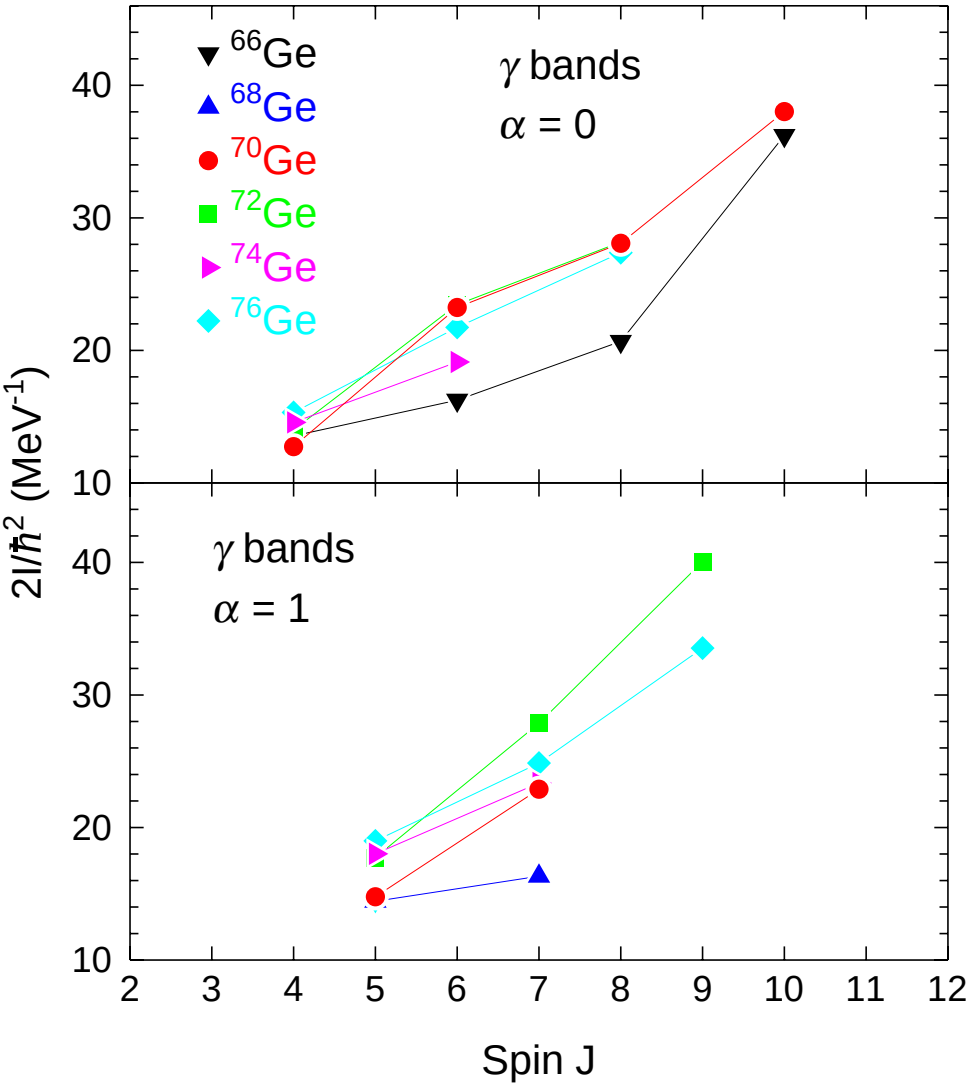

FIG. 7: (Color online) Static moment-of-inertia parameter $\mathcal{I}$ as a function of spin J for the γ-vibrational bands in ^{66}Ge [17], ^{68}Ge [18], ^{70}Ge, ^{72}Ge [3], ^{74}Ge [45], and ^{76}Ge [1].

Evidence suggests that this structure is triaxial-deformed and γ soft, consistent with the expectation for the lowest positive-parity states from TRS calculations. Within the broad valley encompassing the lowest energies of the TRS plots at low frequency (similar to what is shown in the top panel of Fig. 5) is a secondary collective minimum at $\beta_2 \approx 0.23$ and $\gamma \approx -35^\circ$ that begins to develop at $\hbar\omega \approx 0.2$ MeV, which could represent the lowest states of

the γ band. An experimental signature of triaxial deformation is the observation of several interband transitions with other structures since triaxiality introduces significant mixing between different K values. Indeed, several linking transitions have been observed between the γ band and other positive-parity bands, pointing to possible underlying triaxiality.

The degree of γ rigidity can be explored within the context of the $S(J)$ energy staggering parameter, defined by [48]

$$S(J) = \frac{[E(J) - E(J-1)] - [E(J-1) - E(J-2)]}{E(2_1^+)}. \quad (3)$$

The $S(J)$ parameter quantifies the grouping of adjacent levels according to their energy, and provides insight into the degree of γ-shape rigidity based on its phase [48]. As shown in Fig. 8, the staggering pattern deduced for the γ band in ^{70}Ge highly resembles those of the γ bands in several other neighboring Ge isotopes, with a phase that strongly suggests a γ-soft shape. Although a change of phase in the pattern of $S(J)$ occurs at $J = 6$ in ^{74}Ge [45], only the oscillations of $S(J)$ for ^{76}Ge indicate a phase opposite to that of the other neighboring even-even Ge isotopes throughout the entire observable range of the γ band, representing a very rare instance of a γ-rigid shape at low excitation energy [1].

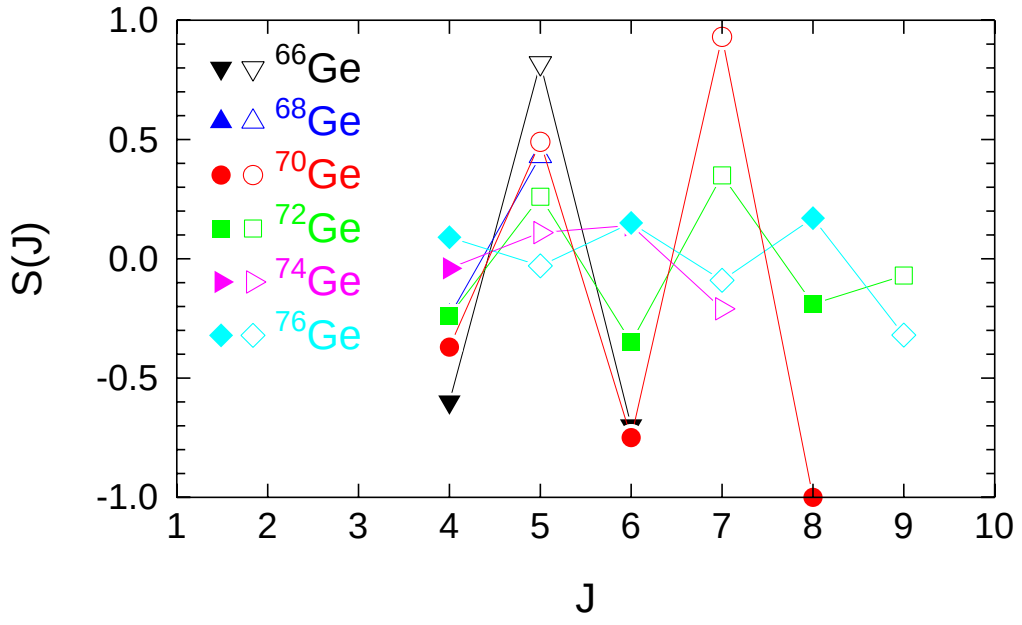

FIG. 8: (Color online) Energy staggering parameter $S(J)$ as a function of spin J for the γ-vibrational bands in ^{66}Ge [17], ^{68}Ge [18], ^{70}Ge, ^{72}Ge [3], ^{74}Ge [45], and ^{76}Ge [1]. Filled (open) symbols represent $S(J)$ values associated with even (odd) J.

C. Negative-parity bands

The 3^- state at 2562 keV has been associated with an octupole vibration based on its excitation energy [12] as well as its considerable $B(E3)$ decay strength of 42(6) W.u.[43, 49]. These characteristics match the systematic behavior demonstrated by octupole vibrational states in other even-even Ge isotopes [3, 50, 51]. Other low-lying yrast states with negative parity have generally been associated with $\nu(fp \otimes g_{9/2})$ configurations [11, 12], although some of these states have also been interpreted within the context of a two-proton cluster-vibration coupling model [13]. Significant mixing has been proposed among the low-lying negative-parity states in ^{66}Ge [17] and ^{68}Ge [37] based on the many linking transitions observed between these states. Strong mixing is also likely taking place in ^{70}Ge given the similar complexity of decay branches that exist.

The observed high-spin band based on the 3^- octupole state has been compared to the results of shell-model calculations using various effective interactions [15, 26], which generally revealed satisfactory agreement between the measured and predicted excitation energies. In the present work, the observation of a new 9^- state at 5415 keV within this band (band (4) in Fig. 1) typically resulted in shifting the experimental levels with $J \geq 9$ within about $\pm$150 keV of their previous values [15], leaving their comparison with the shell-model calculations largely unchanged. A notable exception is the energy of the 13_1^- state, which is now about 500 keV higher than that reported in Ref. [15]. This increase in excitation energy provides better agreement with the corresponding values predicted by shell-model calculations using the G-matrix and EPQQM effective interactions [15], but results in somewhat worse agreement with shell-model results using the PMMU interaction [26].

Previously, the behavior of the experimental spins with rotational frequency in this band suggested a band crossing near the 13_1^- state ($\hbar\omega \approx 0.6$ MeV), attributed to a $\pi(g_{9/2}) \otimes \nu(g_{9/2})^2$ alignment and (presumably) a $\pi(fp \otimes g_{9/2})^2 \otimes \nu(g_{9/2})^2$ 4-qp configuration based on the expectation values of the spin and isospin of nucleons in the $g_{9/2}$ orbit from shell-model calculations [15]. The same shell-model calculations favored the alignment occurring at somewhat higher spin, however. In the present study, the insertion of a new $9_2^- \rightarrow 7_3^-$ 1115-keV transition into this band essentially maintains the same alignment frequency ($\hbar\omega \approx 0.6$ MeV), as demonstrated in the top panel of Fig. 9 by the sharp backbend in $J^{(1)}$ near this frequency. Comparisons among the $J^{(1)}$ spectra for the analogous bands

in neighboring even-even Ge isotopes reveal very similar behaviors, possibly pointing to similar underlying configurations. In fact, the first band crossing observed for this structure in ^{66}Ge was also associated with the aligned $\pi(fp \otimes g_{9/2})^2 \otimes \nu(g_{9/2})^2$ configuration above the 15^- state [17], similar to the conclusions drawn from cranked Nilsson-Strutinski model calculations performed for the analogous band structure in ^{68}Ge [18]. A notable difference among the common features in these $J^{(1)}$ trends is the frequency of the first alignment, which systematically decreases with increasing N, much like the behavior of $J^{(1)}$ for the yrast positive-parity bands in these same isotopes (see Fig. 6).

Figure 10 shows representative results of TRS calculations performed for odd-spin negative-parity states. In these samples, the af configuration (using the qp labeling convention given in Ref. [52]) was chosen for quasiprotons, while the vacuum configuration was used for quasineutrons, resulting in a two-quasiproton configuration that yields the lowest $\alpha = 1$ negative-parity states available in the calculations which might correspond to band (4) in ^{70}Ge. As in the case of the lowest positive-parity states (Fig. 5), the surfaces indicate substantial γ softness with multiple competing minima at $\hbar\omega = 0$ MeV (top panel of Fig. 10), consistent with the picture of strong band mixing that might be expected given the many different linking transitions between band (4) and other structures. The absolute minimum at this frequency occurs at a spin of $J \approx 4$, in fair agreement with the observed band head spin of $J = 3$. A more well-defined non-collective minimum emerges at $\hbar\omega = 0.5$ MeV (middle panel), just below the first band crossing at $\hbar\omega \approx 0.6$ MeV, and persists up to $\hbar\omega = 0.7$ MeV. At a frequency of 0.8 MeV, approximately corresponding to $J = 19$ (the highest observed spin in band (4)), only a rather steep non-collective minimum at $\gamma = 60°$ is evident (bottom panel). The lack of clear collective minima implies relatively longer-lived states in band (4) ($\tau \gtrsim 1$ ps), and might explain why the intraband transitions did not show a noticeable Doppler-shifted line shape at 35° and 145°. TRS calculations that also produce odd-spin negative-parity states, but instead assume two-quasineutron character (the AF configuration [52]), yield somewhat similar results, except that a shallow, near-triaxial minimum with $(\beta_2, \gamma) \approx (0.27, -27°)$ becomes energetically preferred at $\hbar\omega = 0.3$ MeV. This collective minimum diminishes in favor of only non-collective minima above $\hbar\omega = 0.6$ MeV.

The new even-spin negative-parity band (band (5) in Fig. 1) shows characteristics similar to other analogous sequences in neighboring Ge isotopes. Its energy spacings relative to

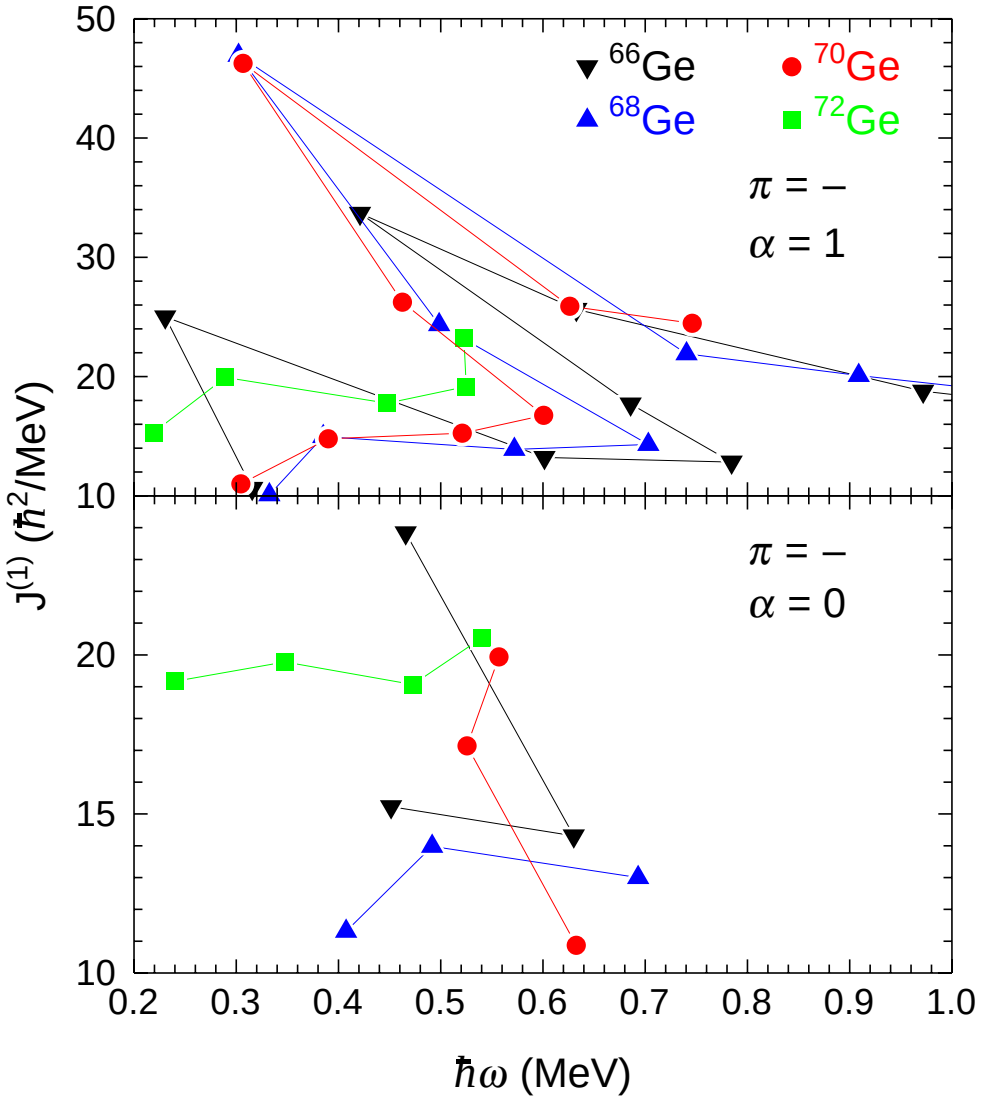

FIG. 9: (Color online) Experimental kinematic moments of inertia $J^{(1)}$ as a function of rotational frequency for the negative-parity bands based on the 3^- octupole state (top panel), as well as for the lowest even-spin negative-parity bands (bottom panel), in ^{66}Ge [17], ^{68}Ge [18], ^{70}Ge, and ^{72}Ge [3]. A common value of $K = 3$ was used in each band.

the more strongly-populated band (4) reveals a signature-splitting pattern that suggests an interpretation as the unfavored signature partner to band (4). The spectrum of $J^{(1)}$ with rotational frequency for this band is dissimilar to that of other unfavored $\alpha = 0$ negative-parity bands in the neighboring Ge isotopes (see Fig. 9), with no systematic pattern evident among them. Such irregular behavior could be another indication of strong configuration mixing between the $f_{5/2}$ and $p_{3/2}$ orbitals near the Fermi surface. TRS calculations for the

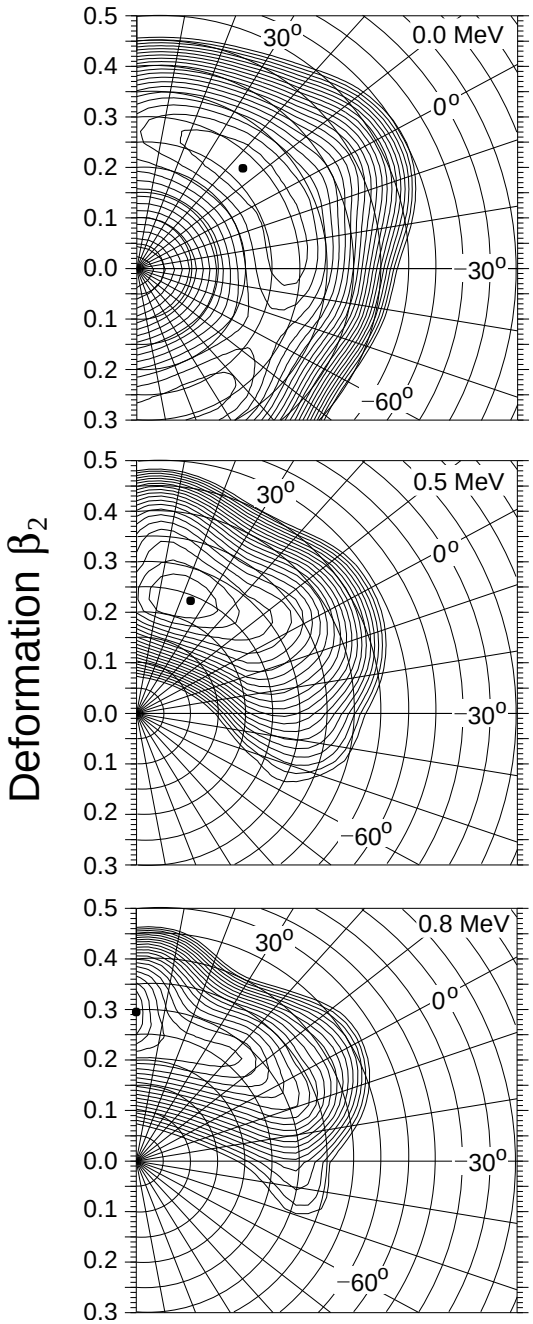

FIG. 10: Sample total Routhian surfaces in the (β_2, γ) plane for the lowest two-quasiproton configuration in ^{70}Ge representing states with $\pi = -$ and $\alpha = 1$ at rotational frequencies of $\hbar\omega = 0$ (top), 0.5 (middle), and 0.8 MeV (bottom). The spacing between contour lines is 200 keV.

lowest $\alpha = 0$, $\pi = -$ states available in the calculations indicate shapes that follow a similar pattern with frequency as the ones for the favored $\alpha = 1$ states.

V. SUMMARY

High-spin states in ^{70}Ge were populated from the ^{55}Mn(^{18}O,$p2n$) reaction at a beam energy of 50 MeV using the John D. Fox Superconducting Accelerator Facility at Florida State University. A Compton-suppressed Ge array consisting of three Clover detectors and seven single-crystal detectors was used to detect γ rays in prompt coincidence.

Our investigation of the high-spin decay of ^{70}Ge resulted in the assignment of 31 new transitions and a rearrangement of four others when compared to the two most recently published works, enhancing the known level scheme with both positive- and negative-parity states organized into multiple band structures. The energies and intensities of all observed transitions in ^{70}Ge were measured, and spin-parity assignments were made based on directional correlation of oriented nuclei (DCO) ratios coupled with transition probability arguments. The ground-state band was observed to fork into two distinct bands above the 6_1^+ state in agreement with previous studies, but the continuation of the band based on the 8_2^+ state has been modified compared to the most recent published work. Two new transitions have been added to the γ-vibrational band, extending it to a 10_3^+ level. The band observed to the highest spin in this work, based on a 3^- octupole state, has been modified to include a new 9_2^- state. Its likely signature partner band has been identified for the first time up to a (12^-) state.

The forking behavior in the ground-state band has been attributed to two separate $(\nu g_{9/2})^2$ alignments with similar band-crossing frequencies, in agreement with the most recent study. Total Routhian surface (TRS) calculations indicated significant insensitivity to the γ triaxiality parameter at low spin for the lowest positive-parity states, with some shape polarization toward prolate deformation evident just above the band-crossing frequency. The γ-vibrational band also shows the classic features of a γ-soft structure based on the behavior of the $S(J)$ energy staggering parameter. These characteristics of the observed positive-parity bands in ^{70}Ge are very similar to those observed in many of the neighboring even-even Ge isotopes and show reasonable agreement with recent shell-model calculations.

The band based on the 3^- octupole state appears to be vibrational in nature near the band head, coupled to either a two-quasineutron or two-quasiproton structure. The kinematic moments of inertia associated with this band indicate a gradual alignment toward a somewhat higher frequency than what was observed previously, providing better agree-

ment with recent triaxial projected shell-model calculations and pointing to a 4-quasiparticle structure likely based on the $\pi(fp \otimes g_{9/2})^2 \otimes \nu(g_{9/2})^2$ configuration. TRS calculations for both favored and unfavored negative-parity states paint a picture of significant γ softness and shapes that favor non-collective degrees of freedom across the range of observed spins.

Acknowledgments

This work was supported in part by the U. S. National Science Foundation through Grant No. PHY-10-64819 (FSU) and Research Experience for Undergraduates (REU) Program Grant No. 1262850 (OWU), as well as the Ohio Wesleyan University Summer Science Research Program. Three authors (P.R.P.A., N.H.M., and J.R.B.O.) acknowledge financial support from the Brazilian agencies CNPq and FAPESP. We are grateful to the staff of the FSU John D. Fox Superconducting Accelerator Facility for their support throughout the experiment, and to W. Nazarewicz for providing the results of his cranked Woods-Saxon calculations. Figure 1 for this article was created using the LevelScheme scientific figure preparation system [M. A. Caprio, Comput. Phys. Commun. **171**, 107 (2005), http://scidraw.nd.edu/levelscheme].

---

[1] Y. Toh, C. J. Chiara, E. A. McCutchan, W. B. Walters, R. V. F. Janssens, M. P. Carpenter, S. Zhu, R. Broda, B. Fornal, B. P. Kay, F. G. Kondev, W. Królas, T. Lauritsen, C. J. Lister, T. Pawlat, D. Seweryniak, I. Stefanescu, N. J. Stone, J. Wrzesiński, K. Higashiyama, and N. Yoshinaga, Phys. Rev. C **87**, 041304(R) (2013).

[2] A. D. Ayangeakaa, R. V. F. Janssens, C. Y. Wu, J. M. Allmond, J. L. Wood, S. Zhu, M. Albers, S. Almaraz-Calderon, B. Bucher, M. P. Carpenter, C. J. Chiara, D. Cline, H. L. Crawford, H. M. David, J. Harker, A. B. Hayes, C. R. Hoffman, B. P. Kay, K. Kolos, A. Korichi, T. Lauritsen, A. O. Macchiavelli, A. Richard, D. Seweryniak, and A. Wiens, Phys. Lett. B **754**, 254 (2016).

[3] D. G. Roux, K. R. Henninger, R. A. Bark, S. Bvumbi, E. A. Gueorguieva-Lawrie, J. J. Lawrie, S. M. Mullins, S. H. T. Murray, S. S. Ntshangase, L. P. Masiteng, and O. Shirinda, Eur. Phys. J. A **48**, 99 (2012).

[4] J. Dudek, A. Goźdź, N. Schunck, and M. Miśkiewicz, Phys. Rev. Lett. **88**, 252502 (2002).

[5] K. C. Chung, A. Mittler, J. D. Brandenberger, and M. T. McEllistrem, Phys. Rev. C **2**, 139 (1970).

[6] K. R. Alvar and S. Raman, Nucl. Data Sheets **8**, 1 (1972).

[7] G. C. Ball, R. Fournier, J. Kroon, T. H. Hsu, and B. Hird, Nucl. Phys. A **231**, 334 (1974).

[8] D. Ardouin, R. Tamisier, M. Vergnes, G. Rotbard, J. Kalifa, G. Berrier, and B. Grammaticos, Phys. Rev. C **12**, 1745 (1975); D. Ardouin, Ph. D. thesis, Université de Nantes, 1975.

[9] J. P. Labrie, E. E. Habib, and Z. Preibisz, Can. J. Phys. **53**, 117 (1975).

[10] Li Yan, Shen Shuifa, Shi Shuanghui, Gu Jiahui, Yu Xiaohan, Liu Jingyi, and Zeng Jiping, Appl. Rad. Iso. **57**, 399 (2002).

[11] C. Morand, M. Agard, J. F. Bruandet, A. Giorni, J. P. Longequeue, and Tsan Ung Chan, Phys. Rev. C **13**, 2182 (1976).

[12] R. L. Robinson, H. J. Kim, R. O. Sayer, J. C. Wells, Jr., R. M. Ronningen, and J. H. Hamilton, Phys. Rev. C **16**, 2268 (1977).

[13] L. Cleemann, J. Eberth, W. Neumann, and V. Zobel, Nucl. Phys. A **386**, 367 (1982).

[14] B. Mukherjee, S. Muralithar, G. Mukherjee, R. P. Singh, R. Kumar, J. J. Das, P. Sugathan, N. Madhavan, P. V. Madhusudanan Rao, A. K. Sinha, G. Shanker, S. L. Gupta, D. Mehta, S. L. Katoch, C. R. Praharaj, A. K. Pande, L. Chaturvedi, S. C. Pancholi, and R. K. Bhowmik, Acta Phys. Hung. New Ser.: Heavy Ion Phys. **13**, 253 (2001).

[15] M. Sugawara, Y. Toh, M. Oshima, M. Koizumi, A. Kimura, A. Osa, Y. Hatsukawa, H. Kusakari, J. Goto, M. Honma, M. Hasegawa, and K. Kaneko, Phys. Rev. C **81**, 024309 (2010).

[16] M. Kumar Raju, P. V. Madhusudhana Rao, S. Muralithar, R. P. Singh, G. H. Bhat, J. A. Sheikh, S. K. Tandel, P. Sugathan, T. Seshi Reddy, B. V. Thirumala Rao, and R. K. Bhowmik, Phys. Rev. C **93**, 034317 (2016).

[17] E. A. Stefanova, I. Stefanescu, G. de Angelis, D. Curien, J. Eberth, E. Farnea, A. Gadea, G. Gersch, A. Jungclaus, K. P. Lieb, T. Martinez, R. Schwengner, T. Steinhardt, O. Thelen, D. Weisshaar, and R. Wyss, Phys. Rev. C **67**, 054319 (2003).

[18] D. Ward, C. E. Svensson, I. Ragnarsson, C. Baktash, M. A. Bentley, J. A. Cameron, M. P. Carpenter, R. M. Clark, M. Cromaz, M. A. Deleplanque, M. Devlin, R. M. Diamond, P. Fallon, S. Flibotte, A. Galindo-Uribarri, D. S. Haslip, R. V. F. Janssens, T. Lampman, G. J.

Lane, I. Y. Lee, F. Lerma, A. O. Macchiavelli, S. D. Paul, D. Radford, D. Rudolph, D. G. Sarantites, B. Schaly, D. Seweryniak, F. S. Stephens, O. Thelen, K. Vetter, J. C. Waddington, J. N. Wilson, and C.-H. Yu, Phys. Rev. C **63**, 014301 (2000).

[19] J. Pavan, Ph. D. thesis, Florida State University, 2003.

[20] [http://fsunuc.physics.fsu.edu/~caussyn/].

[21] Table of Isotopes, ed. R. B. Firestone and V. S. Shirley, Eighth Edition (Wiley-Interscience, New York, 1996).

[22] E. F. Moore, P. D. Cottle, C. J. Gross, D. M. Headly, U. J. Hüttmeier, S. L. Tabor, and W. Nazarewicz, Phys. Rev. C **38**, 696 (1988).

[23] R. A. Haring-Kaye, R. M. Elder, J. Döring, S. L. Tabor, A. Volya, P. R. P. Allegro, P. C. Bender, N. H. Medina, S. I. Morrow, J. R. B. Oliviera, and V. Tripathi, Phys. Rev. C **92**, 044325 (2015).

[24] L. Cleemann, U. Eberth, J. Eberth, W. Neumann, and V. Zobel, Phys. Rev. C **18**, 1049 (1978).

[25] G. A. Dostemesova, D. K. Kaipov, and Yu. G. Kosyak, Proc. 35th Ann. Conf. Nucl. Spectrosc. Struct. At. Nuclei, Leningrad, 60 (1985).

[26] K. Kaneko, T. Mizusaki, Y. Sun, and S. Tazaki, Phys. Rev. C **92**, 044331 (2015).

[27] S. J. Q. Robinson, L. Zamick, and Y. Y. Sharon, Phys. Rev. C **83**, 027302 (2011).

[28] A. Corsi, J.-P. Delaroche, A. Obertelli, T. Baugher, D. Bazin, S. Boissinot, F. Flavigny, A. Gade, M. Girod, T. Glasmacher, G. F. Grinyer, W. Korten, J. Libert, J. Ljungvall, S. McDaniel, A. Ratkiewicz, A. Signoracci, R. Stroberg, B. Sulignano, and D. Weisshaar, Phys. Rev. C **88**, 044311 (2013).

[29] G. H. Bhat, W. A. Dar, J. A. Sheikh, and Y. Sun, Phys. Rev. C **89**, 014328 (2014).

[30] W. Nazarewicz, J. Dudek, R. Bengtsson, T. Bengtsson, and I. Ragnarsson, Nucl. Phys. A **435**, 397 (1985).

[31] K. J. Weeks, T. Tamura, T. Udagawa, and F. J. W. Hahne, Phys. Rev. C **24**, 703 (1981).

[32] P. D. Duval, D. Goutte, and M. Vergnes, Phys. Lett. **124B**, 297 (1983).

[33] A. Petrovici, K. W. Schmid, F. Grümmer, Amand Faessler, and T. Horibata, Nucl. Phys. A **483**, 317 (1988).

[34] R. Lecomte, M. Irshad, S. Landsberger, P. Paradis, and S. Monaro, Phys. Rev. C **22**, 1530 (1980).

[35] R. Wyss, A. Granderath, R. Bengtsson, P. von Brentano, A. Dewald, A. Gelberg, A. Gizon, J. Gizon, S. Harrissopulos, A. Johnson, W. Lieberz, W. Nazarewicz, J. Nyberg, and K. Schiffer, Nucl. Phys. A **505**, 337 (1989).

[36] L. K. Peker (unpublished).

[37] A. P. de Lima, A. V. Ramayya, J. H. Hamilton, B. Van Nooijen, R. M. Ronningen, H. Kawakami, R. B. Piercey, E. de Lima, R. L. Robinson, H. J. Kim, L. K. Peker, F. A. Rickey, R. Popli, A. J. Caffrey, and J. C. Wells, Phys. Rev. C **23**, 213 (1981); Phys. Rev. C **23**, 2380 (1981).

[38] L. Chaturvedi, X. Zhao, A. V. Ramayya, J. H. Hamilton, J. Kormicki, S. Zhu, C. Girit, H. Xie, W.-B. Gao, Y.-R. Jiang, A. Petrovici, K. W. Schmid, Amand Faessler, N. R. Johnson, C. Baktash, I. Y. Lee, F. K. McGowan, M. L. Halbert, M. A. Riley, J. H. McNeill, M. O. Kortelahti, J. D. Cole, R. B. Piercey, and H. Q. Jin, Phys. Rev. C **43**, 2541 (1991).

[39] U. Hermkens, F. Becker, J. Eberth, S. Freund, T. Mylaeus, S. Skoda, W. Teichert, and A. von der Werth, Z. Phys. A **343**, 371 (1992).

[40] A. Petrovici, K. W. Schmid, F. Grümmer, and Amand Faessler, Nucl. Phys. A **504**, 277 (1989).

[41] A. Petrovici, K. W. Schmid, F. Grümmer, and Amand Faessler, Nucl. Phys. A **517**, 108 (1990).

[42] M. E. Barclay, L. Cleemann, A. V. Ramayya, J. H. Hamilton, C. F. Maguire, W. C. Ma, R. Soundranayagam, K. Zhao, A. Balanda, J. D. Cole, R. B. Piercey, A. Faessler, and S. Kuyucak, J. Phys. G **12**, L295 (1986).

[43] G. Gürdal and E. A. McCutchan, Nucl. Data Sheets **136**, 1 (2016).

[44] Samuel S. M. Wong, *Introductory Nuclear Physics*, Second Ed. (Wiley, New York, 1998).

[45] J. J. Sun, Z. Shi, X. Q. Li, H. Hua, C. Xu, Q. B. Chen, S. Q. Zhang, C. Y. Song, J. Meng, X. G. Wu, S. P. Hu, H. Q. Zhang, W. Y. Liang, F. R. Xu, Z. H. Li, G. S. Li, C. Y. He, Y. Zheng, Y. L. Ye, D. X. Jiang, Y. Y. Cheng, C. He, R. Han, Z. H. Li, C. B. Li, H. W. Li, J. L. Wang, J. J. Liu, Y. H. Wu, P. W. Luo, S. H. Yao, B. B. Yu, X. P. Cao, and H. B. Sun, Phys. Lett. B **734**, 308 (2014).

[46] J. H. Hamilton, R. L. Robinson, and A. V. Ramayya, *Conference on Nuclear Interactions, Canberra, Australia*, in *Lect. Notes Phys.* Vol. **92**, 253 (Springer, Berlin, Heidelberg, 1978).

[47] Mitsuo Sakai and A. C. Rester, At. Data Nucl. Data Tables **20**, 441 (1977).

[48] N. V. Zamfir and R. F. Casten, Phys. Lett. B **260**, 265 (1991).

[49] A. A. Khomich, N. G. Shevchenko, A. Yu. Buki, B. V. Mazanko, V. I. Polishchuck, and Yu. N. Ranyuk, Yad. Fiz. **51**, 27 (1990); Sov. J. Nucl. Phys. **51**, 17 (1990).

[50] F. Ballester, E. Casal, and J. B. A. England, Nucl. Phys. A **490**, 227 (1988).

[51] Der-San Chuu, S. T. Hsieh, and H. C. Chiang, Phys. Rev. C **47**, 183 (1993).

[52] R. Wyss, F. Lidén, J. Nyberg, A. Johnson, D. J. G. Love, A. H. Nelson, D. W. Banes, J. Simpson, A. Kirwan, and R. Bengtsson, Nucl. Phys. A **503**, 244 (1989).

TABLE I: Transition energies (E_γ), spin-parity assignments for the initial (J_i^π) and final (J_f^π) state, relative intensities (I_γ), DCO ratios ($R_{\rm DCO}$), multipolarities (σL), and parent-state excitation energies (E_x) associated with the γ rays observed from the high-spin decay of ^{70}Ge.

E_γ (keV)	J_i^π	J_f^π	I_γ[1]	$R_{\rm DCO}$	σL	E_x (keV)
250.5(2)	6^-	5_1^-	6.4(5)	0.96(4)	$M1/E2$	3667.4(2)
288.4(1)	7_1^-	6^-	4.8(2)	1.00(4)	$M1/E2$	3955.8(2)
309.6(5)	13_1^-	(12^-)	0.1(1)	0.44(19)	$(M1/E2)$	7622.2(3)
344.3(2)	7_3^-	7_1^-	1.1(3)	1.16(13)	$M1/E2$	4300.0(2)
374.0(3)	7_1^-	5_2^-	0.3(1)		$E2$	3955.8(2)
450.6(4)	8_1^+	6_2^+	0.5(1)	1.26(15)	$E2$	4204.2(3)
455.6(3)	6_2^+	6_1^+	0.2(1)	0.95(14)	$M1/E2$	3753.4(3)
501.2(4)	(7_2^-)	5_2^-	0.3(1)		$(E2)$	4082.7(3)
563.4(6)	9_2^-	$8_1^{(-)}$	0.4(2)	0.57(26)	$M1/E2$	5415.3(2)
565.5(4)	10_3^+	(9^+)	0.3(2)		$(M1/E2)$	5821.3(3)
626.5(3)	15^-	13_1^-	3.8(6)	1.01(5)	$E2$	8248.7(4)
653.5(3)	4_2^+	4_1^+	0.5(1)	0.93(12)	$M1/E2$	2806.6(1)
658.0(4)	7_1^-	6_1^+	1.6(2)	0.53(4)	$E1$	3955.8(2)
665.6(4)	(7_2^-)	5_1^-	0.6(2)		$(E2)$	4082.7(3)
668.4(1)	2_2^+	2_1^+	11.5(6)	0.92(7)	$M1/E2$	1707.9(1)
678.9(5)	8_2^+	6_2^+	0.2(1)		$E2$	4432.2(4)
718.2(3)	7_3^-	5_2^-	0.4(2)		$E2$	4300.0(2)
743.8(1)	3^+	2_2^+	9.8(5)	0.94(4)	$M1/E2$	2451.7(1)
769.6(4)	$8_1^{(-)}$	(7_2^-)	0.4(2)		$(M1/E2)$	4852.3(3)
839.6(1)	13_1^-	12_2^+	1.1(3)	0.54(5)	$E1$	7622.2(3)
854.5(1)	5_1^-	3^-	5.6(8)	1.01(14)	$E2$	3416.9(1)
854.6(4)	3^-	2_2^+	0.3(1)		$E1$	2562.4(1)
883.0(4)	7_3^-	5_1^-	1.8(5)	1.02(11)	$E2$	4300.0(2)

896.5(2)	$8_1^{(-)}$	7_1^-	2.8(10)	1.20(9)	$(M1/E2)$	4852.3(3)
901.8(5)	13_1^-	12_1^+	0.2(1)		$E1$	7622.2(3)
906.6(3)	8_1^+	6_1^+	13.0(13)	0.99(4)	$E2$	4204.2(3)
947.0(4)	6_2^+	4_2^+	1.5(2)	0.99(9)	$E2$	3753.4(3)
953.5(4)	13_1^-	11_2^-	3.5(3)	0.91(6)	$E2$	7622.2(3)
983.0(4)	9_2^-	8_2^+	0.4(2)		$E1$	5415.3(2)
1000.1(4)	10_3^+	8_3^+	0.6(2)	0.98(22)	$E2$	5821.3(3)
1002.1(2)	7_3^-	6_1^+	2.4(5)	0.48(4)	$E1$	4300.0(2)
1019.3(2)	5_2^-	3^-	0.6(2)	1.04(37)	$E2$	3581.7(2)
1039.6(1)	2_1^+	0^+	100(10)[2]	1.06(5)	$E2$	1039.6(1)
1040.1(3)	10_1^+	8_1^+	5.6(11)	1.02(35)	$E2$	5244.3(4)
1049.2(6)	13_1^-	11_1^-	0.4(1)	0.88(22)	$E2$	7622.2(3)
1051.6(2)	(9^+)	8_1^+	1.8(6)		$(M1/E2)$	5255.8(4)
1068.4(3)	8_3^+	6_2^+	0.5(1)	1.05(34)	$E2$	4821.8(4)
1094.4(4)	8_2^-	7_1^-	0.4(2)		$M1/E2$	5050.0(3)
1098.7(1)	4_2^+	2_2^+	4.8(5)	0.97(6)	$E2$	2806.6(1)
1109.5(4)	(10^-)	8_2^-	0.6(2)		$(E2)$	6159.2(4)
1109.6(4)	10_2^+	8_2^+	5.2(10)	1.04(16)	$E2$	5541.8(6)
1113.8(2)	4_1^+	2_1^+	52(8)	0.91(2)	$E2$	2153.4(2)
1115.3(3)	9_2^-	7_3^-	2.4(6)	0.91(25)	$E2$	5415.3(2)
1126.6(3)	11_2^-	10_2^+	0.6(3)		$E1$	6668.6(3)
1134.5(2)	8_2^+	6_1^+	8(2)	1.08(16)	$E2$	4432.2(4)
1136.0(2)	(7^+)	(5^+)	0.4(1)		$(E2)$	4806.3(4)
1144.3(2)	6_1^+	4_1^+	27(4)	0.95(4)	$E2$	3297.7(3)
1153.7(5)	(12^-)	(10^-)	0.9(3)		$(E2)$	7312.9(6)
1178.9(4)	12_1^+	10_2^+	0.6(2)		$E2$	6720.5(5)
1211.1(3)	9_2^-	8_1^+	1.4(3)	0.44(6)	$E1$	5415.3(2)
1218.6(3)	(5^+)	3^+	0.8(2)		$(E2)$	3670.3(3)
1240.6(3)	12_2^+	10_2^+	1.8(6)		$E2$	6782.6(5)
1253.3(2)	11_2^-	9_2^-	4.4(4)	0.95(10)	$E2$	6668.6(3)

1263.7(2)	5_1^-	4_1^+	7.4(7)	0.60(5)	$E1$	3416.9(1)
1273.4(4)	11_1^-	9_1^-	1.9(6)		$E2$	6573.5(5)
1274.0(4)	(17_1^-)	15^-	2.0(5)		$(E2)$	9522.8(6)
1306.2(6)	(10^-)	$8_1^{(-)}$	0.7(2)		$(E2)$	6159.2(4)
1329.9(4)	(13_2^-)	11_1^-	0.5(2)		$(E2)$	7903.4(6)
1344.3(2)	9_1^-	7_1^-	2.1(7)	0.94(17)	$E2$	5300.1(3)
1345.4(8)	(14^+)	12_2^+	0.3(1)		$(E2)$	8127.6(6)
1368.7(4)	11_2^-	9_1^-	0.4(2)		$E2$	6668.6(3)
1372.5(6)	(17_2^-)	15^-	1.1(5)		$(E2)$	9621.2(7)
1382.3(3)	8_2^-	6^-	0.6(2)	1.02(24)	$E2$	5050.0(3)
1389.3(4)	10_3^+	8_2^+	0.4(2)	0.97(24)	$E2$	5821.3(3)
1406.7(8)	(14^+)	12_1^+	0.3(1)		$(E2)$	8127.6(6)
1412.1(4)	3^+	2_1^+	4.7(7)	1.01(16)	$M1/E2$	2451.7(1)
1424.5(4)	11_2^-	10_1^+	0.5(1)		$E1$	6668.6(3)
1428.3(3)	5_2^-	4_1^+	1.4(2)	0.58(12)	$E1$	3581.7(2)
1459.5(5)	9_2^-	7_1^-	0.4(2)		$E2$	5415.3(2)
1476.0(4)	12_1^+	10_1^+	3.5(12)	1.16(24)	$E2$	6720.5(5)
1512.6(8)	(19^-)	(17_1^-)	0.6(2)		$(E2)$	11035.4(10)
1522.8(1)	3^-	2_1^+	11(2)	0.50(4)	$E1$	2562.4(1)
1524.5(6)	8_3^+	6_1^+	0.8(2)		$E2$	4821.8(4)
1538.5(4)	12_2^+	10_1^+	0.6(2)	0.94(28)	$E2$	6782.6(5)
1616.9(3)	10_3^+	8_1^+	0.6(2)	0.91(26)	$E2$	5821.3(3)
1707.9(1)	2_2^+	0^+	9.3(5)	1.02(9)	$E2$	1707.9(1)

[1] Determined at 90° and corrected for angular distribution effects (see text).
[2] Intensities normalized to this transition.